AD-A071 462 DAVID W TAYLOR NAVAL SHIP RESEARCH AND DEVELOPMENT CE--ETC F/G 20/11
EVALUATION OF SOME CRACK TIP FINITE ELEMENTS FOR ELASTOPLASTIC --ETC(U)
JUL 79 P D HILTON, L N GIFFORD

UNCLASSIFIED DTNSRDC-79/052 NL

END
DATE FILMED
9-79
DDC

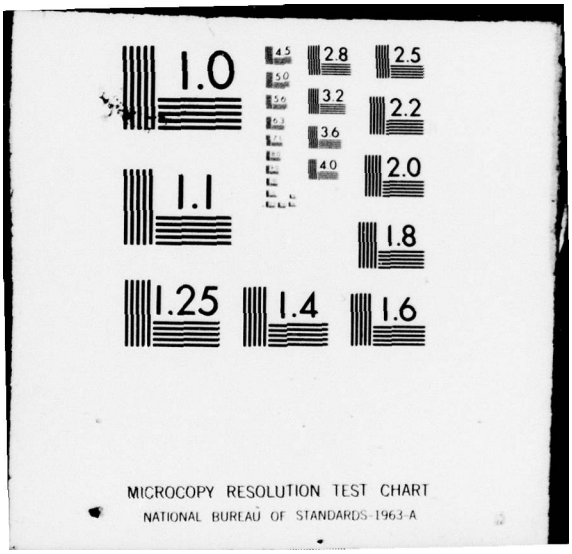
1.0
1.1
1.25
1.4
1.6
1.8
2.0
2.2
2.5
2.8
3.2
3.6
4.0
4.5
5.0
5.6
MICROCOPY RESOLUTION TEST CHART
NATIONAL BUREAU OF STANDARDS-1963-A

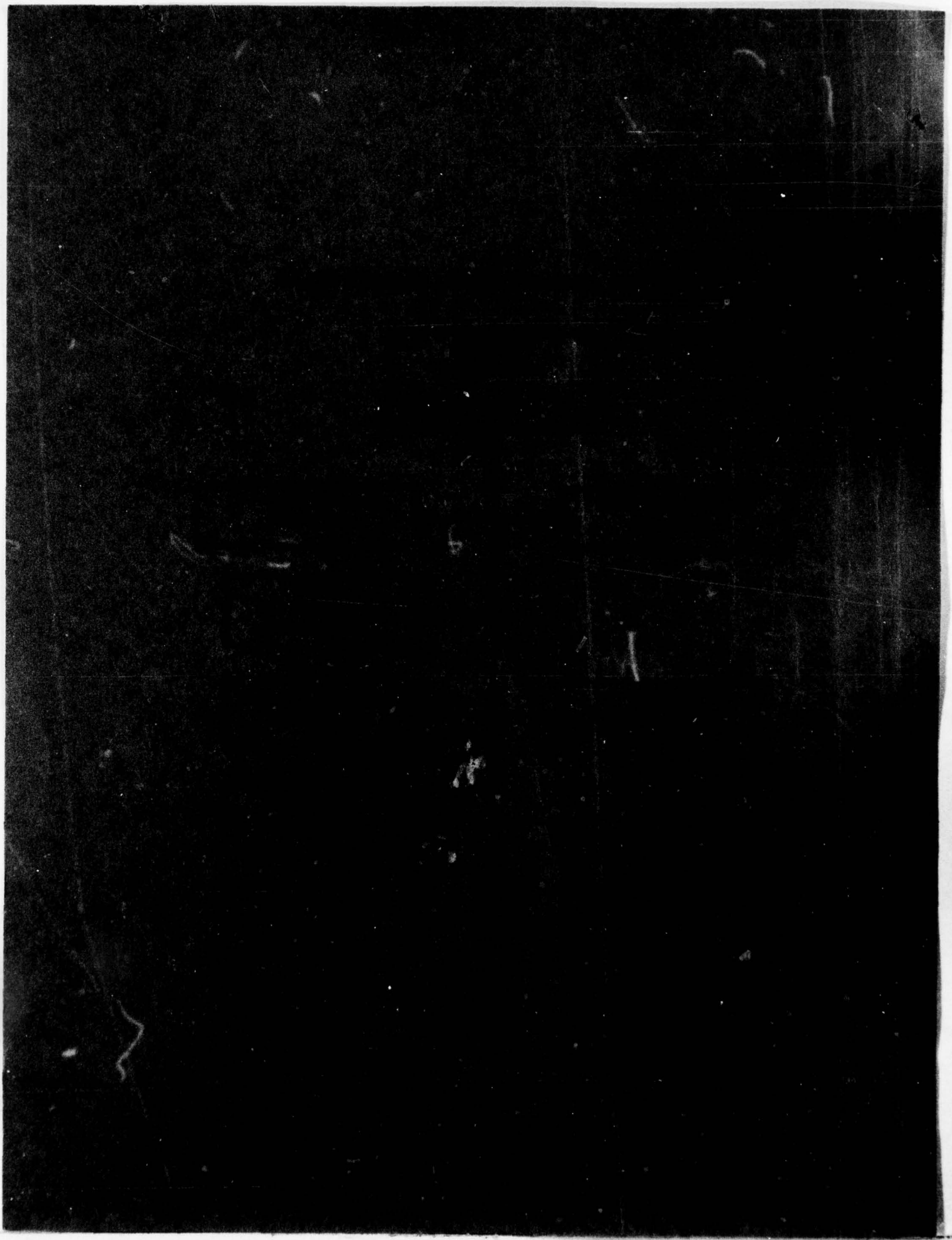

UNCLASSIFIED

SECURITY CLASSIFICATION OF THIS PAGE (When Data Entered)

REPORT DOCUMENTATION PAGE

READ INSTRUCTIONS BEFORE COMPLETING FORM

1. REPORT NUMBER: DTNSRDC-79/052	2. GOVT ACCESSION NO.
3. RECIPIENT'S CATALOG NUMBER	
4. TITLE (and Subtitle): EVALUATION OF SOME CRACK TIP FINITE ELEMENTS FOR ELASTOPLASTIC FRACTURE ANALYSIS	5. TYPE OF REPORT & PERIOD COVERED
	6. PERFORMING ORG. REPORT NUMBER
7. AUTHOR(s): Peter D. Hilton and L. Nash Gifford	8. CONTRACT OR GRANT NUMBER(s)
9. PERFORMING ORGANIZATION NAME AND ADDRESS: David W. Taylor Naval Ship Research and Development Center, Bethesda, Maryland 20084	10. PROGRAM ELEMENT, PROJECT, TASK AREA & WORK UNIT NUMBERS: Program Element 62543N, Project SF 43.422.592, Work Unit 1720-592
11. CONTROLLING OFFICE NAME AND ADDRESS: Naval Sea Systems Command, Washington, D.C. 20362	12. REPORT DATE: July 1979
	13. NUMBER OF PAGES: 36
14. MONITORING AGENCY NAME & ADDRESS (if different from Controlling Office)	15. SECURITY CLASS. (of this report): UNCLASSIFIED
	15a. DECLASSIFICATION/DOWNGRADING SCHEDULE

16. DISTRIBUTION STATEMENT (of this Report)

APPROVED FOR PUBLIC RELEASE: DISTRIBUTION UNLIMITED

17. DISTRIBUTION STATEMENT (of the abstract entered in Block 20, if different from Report)

18. SUPPLEMENTARY NOTES

19. KEY WORDS (Continue on reverse side if necessary and identify by block number)

Fracture Mechanics	Singular Elements
Inelastic Fracture	Numerical Methods
J-integral	Cracked Structures
Finite Element Methods	Plastic Singularity

20. ABSTRACT (Continue on reverse side if necessary and identify by block number)

Specialized nonlinear crack tip finite elements which include the amplitude of the plastic singular solution as an additional unknown are investigated to determine their capability to directly predict the J-integral for cracked elastoplastic bodies without recourse to numerical evaluation of the J-integral over arbitrarily chosen paths. The special elements are used in conjunction with conventional 12-node quadrilateral isoparametric elements.

(Continued on reverse side)

DD FORM 1 JAN 73 1473 EDITION OF 1 NOV 65 IS OBSOLETE S/N 0102-014-6601

UNCLASSIFIED

SECURITY CLASSIFICATION OF THIS PAGE (When Data Entered)

(Block 20 continued)

Power hardening and multilinear representations of the nonlinear stress-strain curve are considered for both deformation and incremental theories of plasticity. Numerical results are presented which demonstrate that the elements fail to provide accurate direct calculation of J, but that they lead to improved estimates of J based on path calculations. It is concluded that special elements at the crack tip improve the accuracy of path values of J, but that the the special elements themselves predict accurate values of J only in materials with high strain hardening slope.

TABLE OF CONTENTS

LIST OF FIGURES

LIST OF TABLES

ABSTRACT

Specialized nonlinear crack tip finite elements which include the amplitude of the plastic singular solution as an additional unknown are investigated to determine their capability to directly predict the J-integral for cracked elastoplastic bodies without recourse to numerical evaluation of the J-integral over arbitrarily chosen paths. The special elements are used in conjunction with conventional 12-node quadrilateral isoparametric elements. Power hardening and multilinear representations of the nonlinear stress-strain curve are considered for both deformation and incremental theories of plasticity. Numerical results are presented which demonstrate that the elements fail to provide accurate direct calculation of J, but that they lead to improved estimates of J based on path calculations. It is concluded that special elements at the crack tip improve the accuracy of path values of J, but that the special elements themselves predict accurate values of J only in materials with high strain hardening slope.

ADMINISTRATIVE INFORMATION

This work was authorized and funded within the Submarine Structures Exploratory Development Program under Program Element 62543N, Project SF 43.422.592, and Work Unit 1720-592.

INTRODUCTION

The finite element calculation of linear elastic stress intensity factors for planar or axisymmetric bodies has become commonplace and highly accurate. Indirect methods, in which conventional elements are forced to display the correct near tip displacement field, have been discussed by Henshell and Shaw,[1*] and by Barsoum[2] for the 8-node quadrilateral isoparametric element, and by Pu et al.[3] for the 12-node quadrilateral isoparametric element. In these methods, a corner node corresponds to the crack tip, and edge nodes adjacent to the tip are moved to the 1/4 position for the 8-node element, or to the 1/9-4/9 positions for the 12-node element, thus imposing the proper $\sqrt{r}$ variation of displacement with respect to

*A complete listing of references is given on page 27.

distance from the crack tip. Stress intensity factors K_I and K_{II} are then calculated based upon examination of nodal displacements in the vicinity of the crack tip.

On the other hand, Hilton and Gifford[4-6] have found that highly accurate elastic stress intensity factors can be calculated using specialized crack tip elements in which the stress intensity factors themselves are carried as unknowns. Special, small, circular "core" crack tip elements joined along their periphery to conventional elements have produced good results. An "enrichment" of conventional 12-node isoparametric elements, as suggested originally by Benzley,[7] has proved even more convenient and has improved accuracy. Both of these approaches have been implemented into the APES computer program[6,8] which employs the 12-node isoparametric quadrilateral as a conventional element.

The extension of embedded singularity finite element techniques to the consideration of elastoplastic crack problems was first proposed by Hilton and Hutchinson.[9] In this work, the core crack tip element was employed to embed the Hutchinson[10] and Rice and Rosengren[11] (HRR) plastic singular solution for Mode I crack problems into a deformation theory finite element formulation. Using this approach, the plastic intensity factor was calculated directly and the J-integral[12] was determined from it. Results were presented for the plane stress problem of a central crack in an infinite domain subject to a uniform remote tensile stress field acting normal to the crack direction. The authors extended this approach to plane strain problems and to the use of high order isoparametric elements instead of previously used constant stress triangles remote from the crack tip. They report results for a number of geometries and characteristics, including boundary influence, for example.[4,13]

In this approach, the core element was thought to be particularly attractive for the following reasons:

1. It was not necessary to select a path, a number of paths, or a "best" path over which to evaluate the J-integral.

2. The J-integral was a direct consequence of the calculation.

3. The J-integral was a first order quantity whose accuracy should be on the order of that of nodal displacements; evaluation of J over some path, on the other hand, involves the second order quantities of strain and stress.

Success in elastic calculations with the enriched 12-node isoparametric element[5] was even more dramatic than with the small core element. Not only were problems considerably easier to idealize, but accuracy of the elastic stress intensity factors was found to be practically insensitive to the size of the enriched elements surrounding the crack tip. (Such was not the case with the core element.) This fact quickly led the authors to almost exclusive use of enriched 12-node elements for elastic fracture computations.

This success, along with dissatisfaction over the limitations imposed by deformation theory plasticity coupled with a power hardening material model, has led the authors to yet another approach to the elastoplastic Mode I crack problem. This took the form of an enriched elastoplastic 12-node isoparametric crack tip element, coupled with conventional 12-node elements, and all formulated using incremental theory plasticity and a multilinear representation of the material stress-strain curve.

From analyzing the results of all of this work, the authors are able to compare the influences of the following in elastoplastic fracture analysis:

1. Different models of material behavior
2. Different near-tip elements (core, enriched, 1/9-4/9 and nonsingular)
3. Path and singularity (direct formulation, first order) predictions of the J-integral

In the following, the development of each of the nonlinear formulations will be outlined, and then numerical results will be compared. It will be concluded that while path calculation of the J-integral is satisfactory using singular elastoplastic elements, the directly calculated singular values themselves are not, in general, accurate. Thus the advantage enjoyed in the use of such elements in the elastic case is lost in the

nonlinear case. The unsatisfactory prediction of singular J values will then be explained and discussion regarding the need for special elements for accurate path prediction will be given.

MATERIAL MODELS AND ASSOCIATED CRACK TIP SINGULARITIES

POWER HARDENING MATERIAL

For a power hardening material, the uniaxial stress-strain law is given by

$$\varepsilon = \frac{1}{E} \begin{cases} \sigma & \text{for } \sigma \leq \sigma_{yp} \\ \sigma - \alpha\sigma_{yp} + \alpha\sigma(\sigma/\sigma_{yp})^{n-1} & \text{for } \sigma > \sigma_{yp} \end{cases} \tag{1}$$

where σ and ε = uniaxial stress and strain

σ_{yp} = the yield stress

E = Young's modulus

α and n = constants chosen such that Equation (1) models the experimental stress-strain curve

For such a material model under conditions of plane stress, plane strain, or axial symmetry, Hutchinson[9] has shown that the near crack tip fields are given for the Mode I case by

$$\sigma_{ij} = K_p r^{-1/n+1} \tilde{\sigma}_{ij}(\theta) \tag{2a}$$

$$\varepsilon_{ij} \approx \varepsilon^p_{ij} = \alpha \frac{K_p^n}{E} r^{-n/n+1} \tilde{\varepsilon}_{ij}(\theta) \tag{2b}$$

$$u_i = u_{io} + \alpha \frac{K_p^n}{E} r^{1/n+1} \tilde{u}_i(\theta) \tag{2c}$$

where σ_{ij}, ε_{ij}, and u_i = stress, strain, and displacement components

r and θ = polar coordinates centered at the crack tip as shown in Figure 1

K_p = the plastic intensity factor

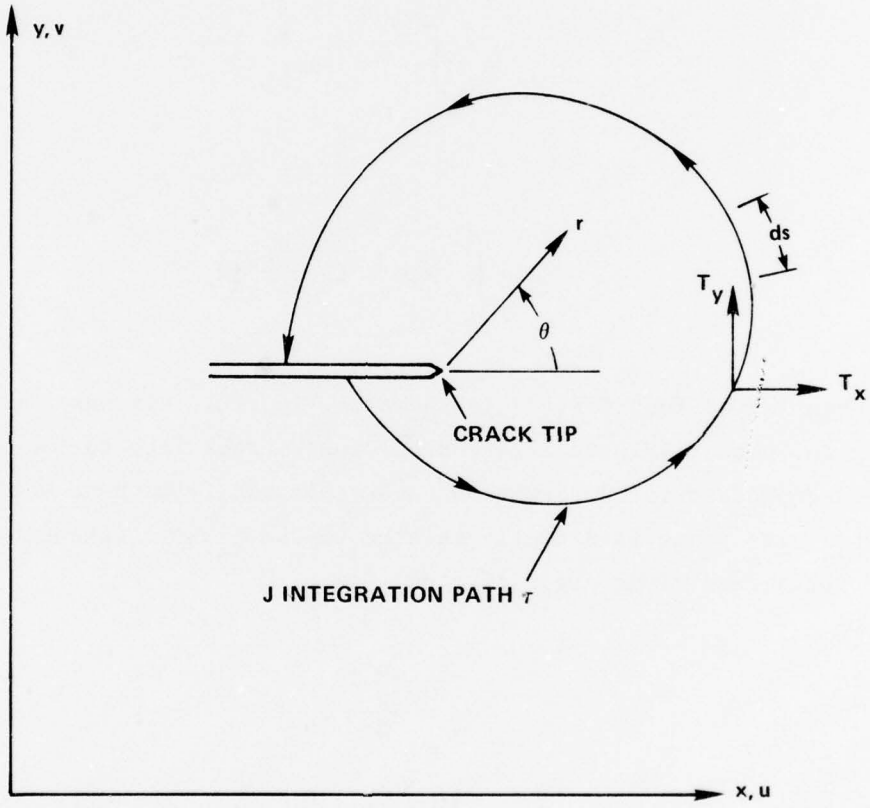

Figure 1 - Polar Coordinate System at Crack Tip and Contour for J Path Integral

The functions $\tilde{\sigma}_{ij}(\theta)$, $\tilde{\varepsilon}_{ij}(\theta)$, and $\tilde{u}_i(\theta)$ are determined by the numerical solution of a nonlinear fourth order ordinary differential equation; they are dependent on the hardening exponent n and are distinct for the cases of plane stress and plane strain. The near-tip fields, Equations (2),

are limited to the region for which plastic strain components ε_{ij}^{p} dominate the corresponding elastic components. Thus the physical region over which Equation (2) applies is a function of applied load and increases in size as the applied load increases.

Rices' J-integral[12] given in terms of the strain-energy density W,

$$W = \int_{0}^{\varepsilon_{mn}} \sigma_{ij} d\varepsilon_{ij} \tag{3}$$

is

$$J = \int_{\tau} W dy - T_i \frac{\partial u_i}{\partial x} ds \tag{4}$$

The notation of Equation (4) is shown in Figure 1. It has been shown that along any path τ (Figure 1), from the lower crack face to the upper, J is path independent for deformation theory plasticity with no unloading. Further, its value is directly related to the plastic intensity factor K_p when these conditions are satisfied, i.e.,

$$J = \frac{K_p^{n+1}}{E} I_n \tag{5}$$

where I_n is a definite integral[10] dependent only on the hardening exponent n.

BILINEAR AND MULTILINEAR MATERIALS

The associated near-tip field found by Hutchinson[10] for bilinear material models has not been employed previously in conjunction with the finite element method to determine J values, etc. For this reason, the description here will contain more detail than that for the power hardening material fully described elsewhere.[4]

The uniaxial multilinear model of material behavior is

$$\varepsilon = \frac{\sigma}{E} + \frac{\alpha_1}{E}(\sigma_1-\sigma_{yp}) + \frac{\alpha_2}{E}(\sigma_2-\sigma_1) + \ldots \frac{\alpha_m}{E}(\sigma-\sigma_{m-1}) \tag{6}$$

where $\sigma_{m-1} < \sigma \leq \sigma_m$ and α_m is defined as $(E\Delta\varepsilon_m-\Delta\sigma_m)/\Delta\sigma_m$. The number of inelastic plastic segments in the material model, N, is greater than or equal to m. The cutoff of the last segment is at infinity, i.e., $\varepsilon_N = \infty$.

The Hutchinson work[10] is based on the special case of bilinear material response, N = 1, and the assumption that the region immediately surrounding the crack tip is yielded. He obtains the asymptotic solution for the Airy stress function

$$\phi = \frac{K_p r^{3/2}}{\sqrt{2\pi}} (\cos\theta/2+1/3\cos 3\theta/2) \tag{7}$$

applicable to both plane stress and plane strain. Thus the plastic singular solution for the near tip stress components has the same (r,θ) dependence as in the elastic case within the yielded zone.

The generalization of Equation (6) for multiaxial stress states is

$$\varepsilon_{ij} = \frac{(1+\nu)}{E}\sigma_{ij} - \frac{\nu}{E}\sigma_{pp}\delta_{ij}$$

$$+ \frac{1.5}{E}\left\{\alpha_m-[(\alpha_1\sigma_{yp})+(\alpha_2-\alpha_1)\sigma_1 + \ldots (\alpha_m-\alpha_{m-1})\sigma_{m-1}]/\sigma_e\right\} s_{ij} \tag{8}$$

when $(\sigma_e)_{m-1} < \sigma_e \leq (\sigma_e)_m$. In the above, ν is Poisson's ratio, δ_{ij} is the Kroneker delta, σ_e is the effective or von Mises stress, s_{ij} is the deviatoric stress tensor, and the α_i are the parameters defining the slopes of the various segments describing the hardening portions of the uniaxial

stress-strain curve. Using Equation (8), the asymptotic stress, strain, and displacement fields within the yielded zone may be obtained from the Airy stress function. The results for the displacement fields are:

$$u = u_o + \frac{K_p}{4E}\sqrt{\frac{2r}{\pi}}\left[\left(5-3\nu+\frac{7}{2}\alpha_N\right)\cos\frac{\theta}{2} - \left(1+\nu+\frac{3}{2}\alpha_N\right)\cos\frac{3\theta}{2}\right] + O(r) \tag{9a}$$

$$v = \frac{K_p}{4E}\sqrt{\frac{2r}{\pi}}\left[\left(7-\nu+\frac{13}{2}\alpha_N\right)\sin\frac{\theta}{2} - \left(1+\nu+\frac{3}{2}\alpha_N\right)\sin\frac{3\theta}{2}\right] + O(r) \tag{9b}$$

for plane stress and

$$u = u_o + \frac{K_p}{4E}\sqrt{\frac{2r}{\pi}}\left[\left(5-3\nu+\frac{7}{2}\alpha_N-8\beta\right)\cos\frac{\theta}{2} - \left(1+\nu+\frac{3}{2}\alpha_N\right)\cos\frac{3\theta}{2}\right] + O(r) \tag{10a}$$

$$v = \frac{K_p}{4E}\sqrt{\frac{2r}{\pi}}\left[\left(7-\nu+\frac{13}{2}\alpha_N-8\beta\right)\sin\frac{\theta}{2} - \left(1+\nu+\frac{3}{2}\alpha_N\right)\sin\frac{3\theta}{2}\right] + O(r) \tag{10b}$$

for the plane strain case with $\beta = (\nu+\alpha_N/2)^2/(1+\alpha_N)$.

The J-integral can be expressed in terms of the plastic intensity factor K_p by carrying out the integration on a path in the region governed by the plastic singularity solution, Equations (9) or (10). The results are

$$J = (1+\alpha_N)\,K_p^2/E \text{ (plane stress)} \tag{11a}$$

$$J = \left[1+\gamma^2/2-1.5\nu\gamma+\alpha_N\left(1-\frac{3\gamma}{4}+\frac{\gamma^2}{2}\right)\right]K_p^2/E \text{ (plane strain)} \tag{11b}$$

with $\gamma = (\nu+\alpha_N/2)\cdot(1+\alpha_N)$

It is important to note that the development of Equations (9) and (10) differs significantly from the corresponding derivation of Equations (2) for the power hardening material in that:

1. Equations (9) and (10) contain the elastic and the plastic contributions to the asymptotic displacement field while Equations (2) contain only the plastic contribution.

2. In Equations (9) and (10), the contributions of order O(r) which are neglected contain the portion of the displacement component derived from the s_{ij}/σ_e term in Equation (8). In other words, the asymptotic solution has been found based on the strain-stress assumption

$$\varepsilon_{ij} = \frac{(1+\nu)}{E}\sigma_{ij} - \frac{\nu}{E}\sigma_{pp}\delta_{ij} + \frac{3}{2E}\alpha_N s_{ij} \qquad (12)$$

SPECIALIZED CRACK TIP ELEMENTS

CORE ELEMENT

A semicircular core element has been developed[4] for elastoplastic Mode I problems in which the assumed displacement field is given by the asymptotic solution, Equations (2), (9), or (10), with unknown parameters u_o (the x displacement component of the crack tip) and K_p. This small special element is connected to standard 12-node isoparametric elements along its periphery by using the last of Equations (2), (9), or (10) as displacement constraints for nodes falling on the boundary. The element thus has a variable number of nodal points; usually, three or four standard 12-node elements adjoin its boundary. The related finite element calculations result in direct predictions of K_p and u_o as well as all nodal displacement components, strains, and stresses. Employing Equations (5), (11a), or (11b), the authors were able to directly calculate the J-integral as an unknown associated with the plastic singular solution. In addition, provision has been made to evaluate J along a path near the crack tip in the first ring of conventional elements around the core element according to Equation (4).

ENRICHED ELEMENT

The concept of enriching the conventional element displacement assumption with the asymptotic displacement field appropriate for fracture analysis originated with Benzley[7] and has been extensively applied for the elastic case by the authors.[5,6] The application described here for the elastoplastic Mode I crack problem is new. In the approach the multilinear material model is used and leading term of the asymptotic expansion for the near-tip crack displacement, Equations (9) or (10), is added to the usual polynomial displacement field within the element. The present application involves enriching 12-node isoparametric elements, i.e.,

$$u = a_1 + a_2 s + a_3 t + a_4 s^2 + \ldots + a_{12} s t^3 + K_p \tilde{u}(s,t)$$

or (13)

$$u = [P]\{a\} + K_p \tilde{u}(s,t)$$

where the "a's" are generalized displacements, (s,t) are the local coordinates associated with the isoparametric element, and $\tilde{u}(s,t)$ represents the term (transformed to local element coordinates) in Equations (9) or (10) in the expression for u whose coefficient is K_p. The expression for the v component of displacement is similar.

Equation (13) is evaluated at each of the twelve nodes to obtain the set of equations for the nodal values of u, i.e., {u}, in terms of the vector {a} as

$$\{u\} = [C]\{a\} + K_p\{\tilde{u}\} \tag{14}$$

Inversion yields

$$\{a\} = [C]^{-1} (\{u\} - K_p\{\tilde{u}\}) \tag{15}$$

Back substitution into Equation (13) gives

$$u = [P][C]^{-1} (\{u\}-K_p\{\tilde{u}\}) + K_p\tilde{u} \tag{16}$$

But from this equation, it is clear that $[P][C]^{-1}$ is nothing more than the set of usual isoparametric shape functions $[N] = [N_1, N_2 \ldots\ldots N_{12}]$. Therefore

$$u = \sum_{i=1}^{12} N_i(s,t)u_i + K_p \left[\tilde{u}(s,t) - \sum_{i=1}^{12} N_i(s,t)\tilde{u}_i\right] \tag{17}$$

and, similarly,

$$v = \sum_{i=1}^{12} N_i(s,t)v_i + K_p \left[\tilde{v}(s,t) - \sum_{i=1}^{12} N_i(s,t)\tilde{v}_i\right] \tag{18}$$

Equations (17) and (18) are the enriched element displacement approximations, giving the displacement components within the element in terms of their nodal values and the plastic intensity factor K_p. The enriched element stiffness matrix is developed from these equations in the usual manner, with the exception that higher order Gauss quadrature (8×8) is employed in the area integration to properly handle the steep gradients near the crack tip.

Implementation of enriched elements of this type into a standard finite element code is not as straightforward as for the core element discussed previously. The enriched element stiffness matrix is of order 25 for the Mode I case, corresponding to 24 unknown nodal displacement components and the singular solution coefficient K_p. Allowance in the construction and solution of the overall stiffness matrix must be made for an additional row and column which correspond to K_p.

The J-integral is calculated from K_p using Equation (11a) or (11b) as described previously. In addition, the J-integral may be evaluated on up to ten different paths specified by the analyst according to Equation (4).

ELEMENT WITH ADJUSTED NODE POSITIONS (1/9-4/9)

Barsoum[14] has shown that when midside nodes of 8-node quadrilateral isoparametric elements are moved to the quarter point nearest the crack tip, a $1/\sqrt{r}$ singularity in the strain field is developed. Following this work, Pu and Hussain[3] found that the same effect could be achieved with 12-node quadrilateral isoparametric elements by moving intermediate nodes to the 1/9 and 4/9 positions nearest the crack tip. The writers have performed elastic calculations with 1/9-4/9 quadrilateral elements (rather than corresponding collapsed triangular elements currently preferred by most investigators) and have obtained highly accurate results. Benzley[15] has shown that the use of quarter point 8-node elements in elastic-plastic computations leads to improved path values of the J-integral. At the same time, the plastic singular solution associated with a multilinear material model contains the square root singularity associated with the 1/9-4/9 element. Thus it became logical to employ the 1/9-4/9 element with a multilinear material model as an additional plastic singularity element.

NUMERICAL EXAMPLES OF J (PATH) VERSUS J (SINGULARITY)

Based on the material described previously, the authors are presently able to make the following calculations:*

1. Calculation of J from the plastic singular solution (hereafter called J_s) of Equation (2) and calculation of J along a path (hereafter called J_p) near the crack tip for a power hardening material using deformation theory plasticity and a small semicircular core crack tip element.

2. The same as above but for a bilinear material model.

---

*These calculations have been made based on elastic-plastic extensions of the APES computer program.[6,8] This nonlinear version of the program has been given the acronym PAPST for Plastic Axisymmetric/Planar STructures. The nonlinear program is still under development and has not yet been formally documented.

3. Calculation of J_s and J_p for bilinear and multilinear material models using incremental plasticity theory and the enriched element whose displacement field is given by Equations (17) and (18).

4. Calculation of J_p as immediately above, but with the use of the 1/9-4/9 elements at the crack tip.

5. Again the same, but with no special treatment of the crack tip.

The hypothetical edge-cracked specimen whose symmetric upper half is shown in Figure 2 is used as an example to illustrate the character of numerical results to be expected. The following material properties were assumed: $E = 30 \times 10^6$ psi (20.7×10^5 Mpa), $\nu = 0.3$, and $\sigma_{yp} = 10^5$ psi (6900 Mpa). The finite element grid patterns are also shown in Figure 2 along with the contours used to evaluate J_p.

Table 1 gives results obtained for the plane strain case using the core element approach and the grid pattern shown in Figure 2b. The core radius r_o in this case is 0.01 in. (0.25 mm) (0.67 percent of crack length). Some of the stress-strain curves for these calculations are shown in Figure 3.

The choice of a small hardening coefficient $\alpha(0.01)$ with a hardening exponent $n = 1$ results in essentially elastic behavior as expected. The J_s and J_p values in this range of material behavior are in close agreement with each other and also with the elastic finite element predictions (J_{ssy}). These excellent predictions are in accordance with the authors' earlier work.[4-6]

Reduced material hardening is handled in the material model by increasing the coefficient α and/or the exponent n. The numerical results given in Table 1 show increasing disparity between J_s and J_p with decreasing strain hardening. Considering a fixed grid pattern and load level, the J_s values first increase slightly and then decrease dramatically as n and/or α is increased. On the other hand, J_p increases monotonically with decreasing strain hardening. The observed numerical dependence of J_s on α and n is not physically realistic. The J_p values, on the other hand, are believed to exhibit the correct trend.

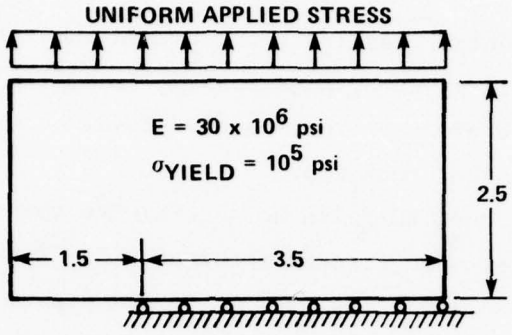

Figure 2a ~ Geometry and Boundary Conditions

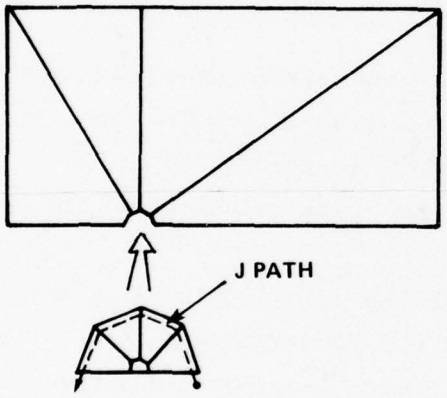

Figure 2b - Nine-Element Mesh

(One Core and Eight Regular)

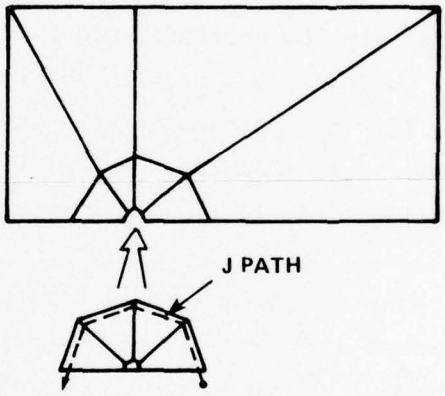

Figure 2c - Thirteen-Element Mesh

(One Core and Twelve Regular)

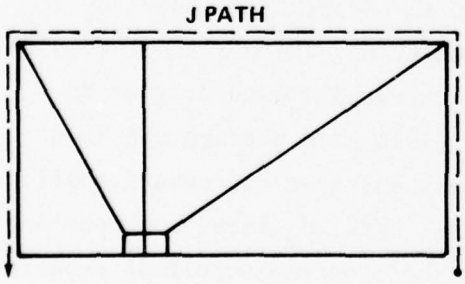

Figure 2d - Six-Element Mesh

(Two Enriched and Four Regular)

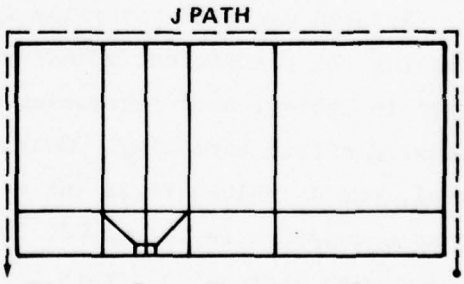

Figure 2e - Fourteen-Element Mesh

(Two Enriched and Twelve Regular)

Figure 2 - Geometry and Idealizations of Hypothetical Edge-Notched Specimen

TABLE 1 - PLANE STRAIN CALCULATIONS FOR POWER HARDENING MODEL FOR VARIOUS VALUES OF n AND α (CORE ELEMENT)

Load (ksi)	J_{ssy}* (Small Scale Yielding) (in-lb/in^2)	n = 1, α = 0.01		n = 1, α = 1		n = 1, α = 10		n = 5, α = 0.01		n = 5, α = 0.5		n = 25, α = 0.01	
		J_s	J_p	J_s	J_p	J_s	J_p	J_s	J_p	J_s	J_p	J_s	J_p
40	851	850	899	762	927	430	1030	1010	926	847	983	701	951
50	1330	1330	1400	1260	1490	774	1760	1540	1410	1370	1650	1110	1630
60	1920	1920	2020	1890	2190	1500	2750	2160	2140	2050	2540	1630	2560
62	2040	2040	2160	2040	2360	1670	3010	2360	2300	2220	2770	1760	2780

NOTES:

1. Core and 8 conventional elements (Figure 2b).
2. Core radius = 0.01 in., σ_{yp} = 100 ksi, E = 30×10^6 psi, ν = 0.3.

*From elastic finite element solution for K_I.

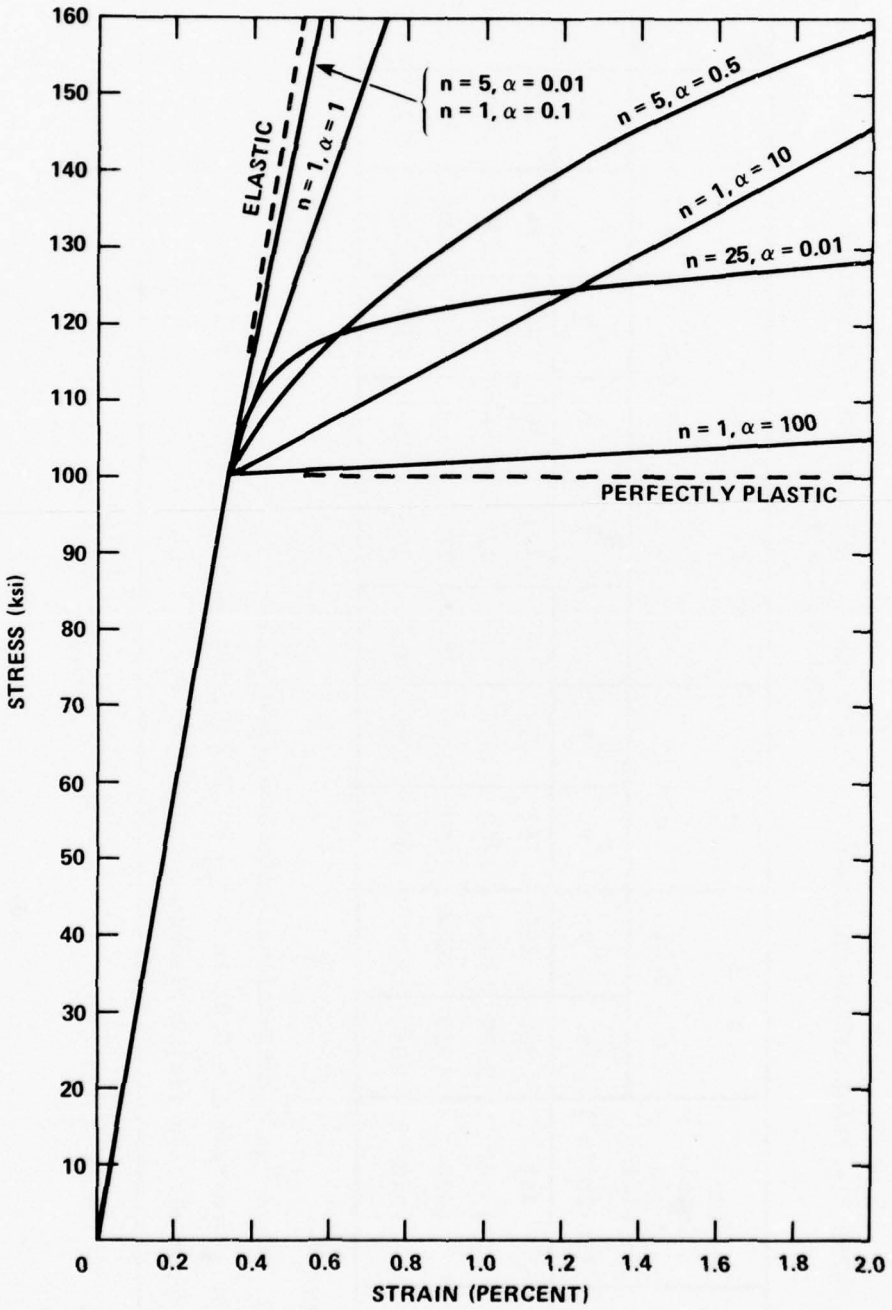

Figure 3 - Typical Stress-Strain Curves Considered in Study

The authors have previously reported numerical predictions for $J = J_s$ [4,9,13] using the circular core element. Those results were for materials with sufficient hardening so that no significant differences in J_s and J_p were observed. It is in the present extension of this approach to lower hardening materials that the discrepancy between J_s and J_p became apparent.

The case for the enriched 12-node element is considered next in the context of a bilinear material model (n=1). As shown in Table 2, when α is very small leading to essentially elastic conditions, the singular and path predictions of J are again in close agreement and also closely agree with the linear elastic finite element results.[6] Again, this was expected based on previous work.

Some of the stress-strain curves assumed in Table 2 are shown in Figure 3. As the hardening coefficient α increases (leading to reduced strain hardening), the difference between J_s and J_p increases, with J_s falling while J_p increases. As α increases beyond about 0.1, the accuracy of the J_s values rapidly decreases. The J_p values, on the other hand, appear to be reasonably accurate over the range of nonlinearity studied.

Table 3 presents results obtained with core element, enriched elements, 1/9-4/9 elements, and conventional element treatments of the crack tip singularity for the cases of plane strain and plane stress. The core element results are from three different grid patterns: 9-element idealization with core radius r_o of 0.02 and 0.01 in. (0.51 and 0.25 mm), and a 13-element idealization with r_o = 0.01 in. (0.25 mm). These grids are shown in Figure 2. The elastic results for $J(J_{ssy})$ exhibit a maximum difference between grid patterns of about 10 percent. This variation is reflected in the plasticity results. The enriched, 1/9-4/9, and conventional treatments of the crack tip shown in Table 3 are for two grid patterns (Figure 2) consisting of 6 and 14 elements. The elastic results show a much weaker dependence of J on grid pattern than that found for the core element. Both enriched idealizations provide elastic results which are more accurate than any of the core element predictions.[4] Thus, the enriched element path values for J_p are believed to be the more accurate of those presented in Table 3.

TABLE 2 - PLANE STRAIN CALCULATIONS FOR BILINEAR MATERIAL MODEL FOR VARIOUS VALUES OF α (ENRICHED ELEMENTS)

Load (ksi)	J_{ssy}* (Small Scale Yielding) (in-lb/in^2)	α = 0.01		α = 0.1		α = 1.0		α = 10		α = 100	
		J_s	J_p	J_s	J_p	J_s	J_p	J_s	J_p	J_s	J_p
6.947	24.9	24.7	24.6	23.9	25.5	13.3	24.5	2.27	24.4	0.24	24.6
40	822	822	815	798	816	620	822	211	835	26	841
50	1280	1280	1270	1260	1280	1040	1310	447	1390	70	1430
60	1850	1850	1840	1820	1850	1610	1940	857	2180	180	2400
62	1980	1980	1960	1950	1970	1740	2080	1000	2440	239	2880

NOTES:

1. 2 enriched and 4 conventional elements (Figure 2d).
2. Strain hardening slope = $E/(1+\alpha)$.
3. σ_{yp} = 100 ksi, $E = 30 \times 10^6$ psi, $\nu = 0.3$.

*From elastic finite element solution for K_I.

TABLE 3 - RESULTS OF DIFFERENT FINITE ELEMENT MODELS FOR BILINEAR MATERIAL BEHAVIOR

TABLE 3A - PLANE STRAIN CALCULATIONS ($E = 30 \times 10^6$, $\nu = 0.3$, $\sigma_{yp} = 10^5$, $\alpha = 10$, $n = 1$)

Load (ksi)	Core Element									Enriched Elements						1/9-4/9		Regular	
	9 Els. $r_o = 0.02$			9 Els. $r_o = 0.01$			13 Els. $r_o = 0.01$			6 Els.			14 Els.			6 Els.	14 Els.	6 Els.	14 Els.
	J_{ssy}*	J_s	J_p	J_{ssy}	J_s	J_p	J_{ssy}	J_s	J_p	J_{ssy}	J_s	J_p	J_{ssy}	J_s	J_p	J_p	J_p	J_p	J_p
40	822	354	980	851	430	1020	771	429	957	814	211	835	811	314	814	838	810	822	801
50	1280	713	1670	1330	774	1760	1200	835	1600	1270	447	1390	1230	636	1330	1390	1320	1350	1310
60	1850	1260	2580	1920	1500	2750	1740	1490	2540	1830	857	2180	1820	1170	2020	2170	2010	2140	1990
62	1980	1400	2820	2040	1610	3010	1850	1640	2780	1960	1000	2440	1950	1330	2230	2430	2220	2360	2190

*J_{ssy} = J integral from elastic finite element solution for K_I.

TABLE 3B - PLANE STRESS CALCULATIONS ($E = 30 \times 10^6$, $\sigma_{yp} = 10^5$, $\alpha = 10$, $n = 1$)

Load (ksi)	Core, 9 Els., $\nu = 0.5$						Enriched 6 Els. $\nu = 0.3$			1/9-4/9 6 Els. $\nu = 0.3$	Regular 6 Els. $\nu = 0.3$
	$r_o = 0.02$			$r_o = 0.01$							
	J_{ssy}*	J_s	J_p	J_{ssy}	J_s	J_p	J_{ssy}	J_s	J_p	J_p	J_p
5.01							12.8	1.39	14.0		
40	903	598	1130	935	733	1150	895	385	1080	1080	1030
50	1410	1300	2190	1550	1720	2230	1400	953	2050	2040	1960
60	2030	2950	3830	2230	3440	3930	2010	1990	3730	3700	3510
62	2170	3530	4450	2380	4080	4530	2130	2460	4410	4360	4090

*J_{ssy} = J integral from elastic finite element solution for K_I.

The following general conclusions are drawn from the results presented in Table 3:

1. Values of J_s are inaccurate for both the core element and enriched elements for materials which exhibit low strain hardening.

2. Values of J_p agree closely for core element (deformation theory plasticity) and enriched element (incremental theory plasticity) idealizations for the plane stress case, but disagree moderately in the plane strain case.

3. For plane strain and plane stress calculations, enriched and 1/9-4/9 elements provide about the same degree of accuracy for J_p values.

4. Inferior values of J_p are obtained when the crack tip is treated in a nonsingular manner. This trend may become much more significant if the path used to calculate J_p is moved closer to the crack tip.

Altogether, the results presented in Tables 1, 2, and 3 lead to two basic conclusions of fundamental importance:

1. Path values J_p may be evaluated with apparently reasonable accuracy for a wide class of stress-strain curves using either the enriched or 1/9-4/9 crack tip elements in conjunction with the incremental theory of plasticity, provided that the chosen path is not very close to the crack tip. This conclusion has limited experimental verification* and has been confirmed analytically by comparison with results obtained in the ASTM-sponsored round-robin J-integral calculation.[16]

2. Singular values J_s are seriously in error for all cases except those involving materials which are nearly elastic. This error occurs with both the core element using deformation theory plasticity and with enriched elements using incremental theory plasticity.

The second conclusion is in contrast to the successful elastic results which prompted this work. The notion that (analogous to the elastic case) J_s could be calculated directly as a first order quantity, independent of path, and with accuracy on the order of that of nodal displacements, has been found to be false. The explanation follows.

---

*This work has been reported informally in DTNSRDC Structures Department Technical Note m-4, "J-integral Analysis of a Compact J_{IC} Specimen," by L. Nash Gifford (Sep 1978).

EXPLANATION OF J (SINGULARITY) RESULTS

For elastic crack problems, the asymptotic expansion of the elastic singular solution about the crack tip has always been convergent over the entire region upon which it has been imposed, i.e., over the core element or over the enriched element. The higher order terms neglected in the elastic singular solution displacement fields become increasingly important with distance from the crack tip; they can apparently be accommodated by the regular contributions to the displacement field in the 12-node enriched element case. For the core element, on the other hand, their importance has been minimized by keeping the element radius at a very small value. Thus, calculations with enriched or core elements in the elastic case have always led to the successful prediction (directly) of the amplitude of the elastic singular solution (K_I or J_{ssy}).

The domain of convergence of the plastic singular solution in elasto-plastic crack problems, however, is limited to a region well within the elastic-plastic boundary, i.e., where the plastic strain contributions dominate the corresponding elastic ones. As an example of how this assumption is easily violated, Figure 4 shows the near-tip finite element mesh (the region within 1/2 in. (12.7 mm) from the crack tip) for the 14-element enriched plane strain test case of Table 3a with $n = 1$ and $\alpha = 10$. The enriched elements for this case are considerably smaller than would be used in the elastic case. Superimposed on the finite element grid in Figure 4 are the elastic-plastic boundaries for various values of the applied remote stress. It can be seen that at an applied remote stress of 20 ksi (138 Mpa), the plastic zone is still quite small and occupies an area less than one-third that of the already relatively small plastically enriched elements surrounding the crack tip. At higher applied stress, the situation improves somewhat, but even at 50 ksi (345 Mpa), one of the enriched elements is not fully within the plastic zone, and neither of the enriched elements are well within the plastic zone. Recall further that the enriched element calculations are based on incremental theory plasticity. Thus the stress state at the higher load increments is dependent on the

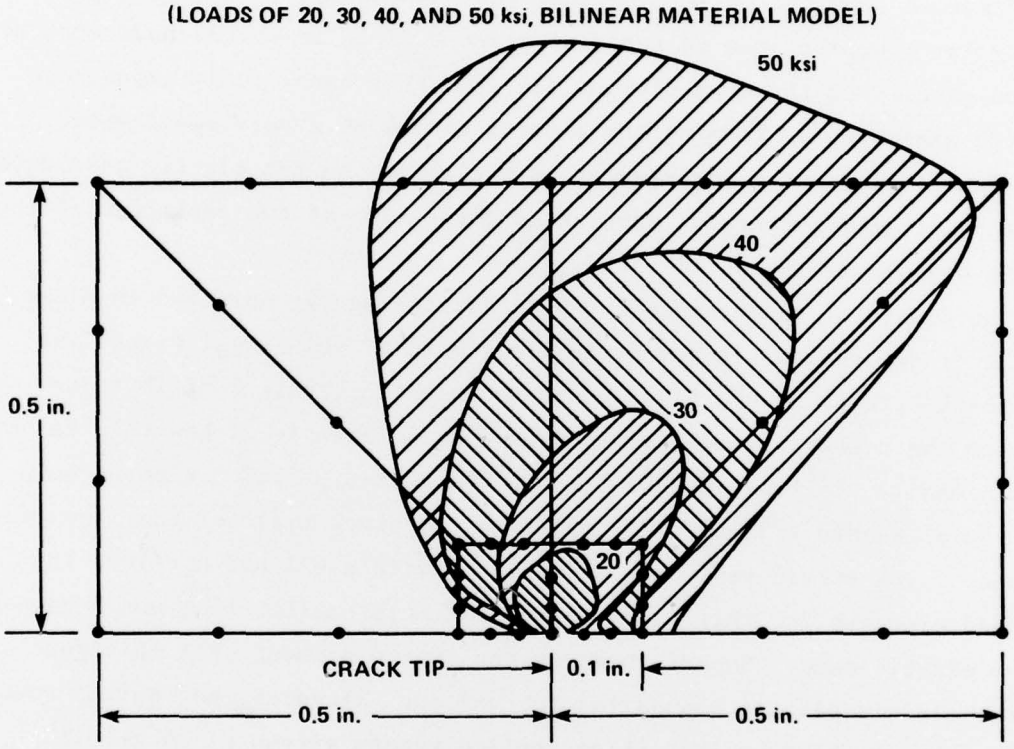

Figure 4 - Elastic-Plastic Interfaces for Fourteen-Element Enriched Test Case of Table 3

stress history, i.e., inconsistencies at lower amplitude loading may propagate to influence the 50 ksi (345 Mpa) load solution. Were the idealization one of plane stress, on the other hand, the plastic zones would be larger at a given load, but still not sufficiently large to enclose the enriched elements well within the plastic zone. The natural tendency would be to overcome this difficulty by drastically decreasing the size of the enriched elements, but that is precisely what this work sought to avoid. Moreover, elastic work[8] indicates a loss of accuracy as enriched element size is made exceedingly small.

We conclude that imposing the plastic singular solution, Equations (2), (9), or (10), over regions which violate the limitation that the plastic singular solution be contained well within the plastic zone leads to incorrect results. Further substantiation of this conclusion can be found by considering the incremental finite element calculations involving enriched elements as reported in Tables 2 and 3b. At low values of applied load, the plastic zone and, therefore, the region of applicability of the plastic singular solution is small. In fact, the magnitude of the lowest load shown in Tables 2 and 3b was chosen so that the most highly stressed quadrature point in the enriched elements is exactly at yield while all others are at or below yield stress. This condition corresponds to small scale yielding, and the elastic singular solution should describe the near field behavior in the enriched elements. For plane stress with $\nu = 0.5$, the asymptotic elastoplastic displacement field, Equation (9), is exactly $(1+\alpha_N)$ times the elastic solution. (Similar, though more complicated, relations hold for $\nu \neq 0.5$ and for plane strain.) If the elastic solution holds, $K_p = K_I/(1+\alpha_N)$ and $J = (1+\alpha_N)K_p^2/E = J_{ssy}/(1+\alpha_N)$. The results in Tables 2 and 3b at the lowest load (first yield) exhibit just this behavior in both the cases of plane strain and plane stress, i.e., $J_s \approx J_{ssy}/(1+\alpha_N)$, and thus support the conclusion that the enriched element is modeling the elastic singularity on the first load increment. As the load increases incrementally, the plastic region spreads to include the entirety of the enriched elements and the value of J_s improves relative to J_p, but not quickly enough to give accurate values within the practical

range of loading considered here. Thus the inconsistency between assumed and actual asymptotic displacement fields imposed at lower load levels persists at higher load levels where the elastoplastic displacement field is likely to be more correct.

The elastoplastic calculations involving the use of the semicircular core element exhibit less discrepancy between J_s and J_p values than the enriched element results. This observation is believed to be a direct consequence of the fact that the core elements employed were significantly smaller in dimension than the corresponding enriched elements. With this exception noted, the poor J_s performance of the core element is explained in like manner.

DISCUSSION AND CONCLUSIONS

Calculations to obtain values of the J-integral for a sample crack problem have been carried out using four different near tip models: the core element, enriched elements, 1/9-4/9 induced singularity elements, and conventional 12-node isoparametric elements. The J values were determined in all cases by path integration (J_p), and by direct calculation of the amplitude of the crack tip singularity (J_s) for core and enriched elements. An aim of this effort was to develop a method for calculating unique J values based on the crack tip singularity and thus avoid the necessity of choosing integration paths and comparing resulting J estimates. The results presented demonstrate failure in reaching that goal; rather, the most reliable J estimates are obtained from path integration based on finite element solutions employing some form of specialized near-tip elements.

Further verification of the accuracy of path values of J calculated using enriched crack tip elements with a multilinear material model has been obtained by comparison with J values from the ASTM round-robin plastic crack problem.[16] The path values of J_p, calculated in this manner, were in the central region of the band of results, leading to increased confidence in the use of the technique. As expected, the corresponding singularity values of $J(J_s)$, as calculated with enriched 12-node elements, were substantially lower than the path values and were outside of the range of other reported results.

In retrospect, the fact that the specialized finite element calculations give accurate path values for J and yet are unable to yield accurate J_s predictions can be explained as follows: The path independence of the J-integral implies a 1/r singularity of the strain energy density function at the crack tip.* The elastic-plastic asymptotic analysis of the two-dimensional crack problem for either a power hardening or a multilinear material model discussed and referenced earlier yields a plastic singular solution which indeed contains a 1/r singularity in strain energy density. The region over which this singularity dominates is, however, dependent on geometry, material behavior (hardening), and applied load amplitude. It is this dependence (of the region of applicability for the plastic singular solution) that has led to the difficulties, discussed earlier, associated with imposing the plastic singular solution on a region (element or elements) and solving for its amplitude J_s. On the other hand, the J path integral, which is a measure of the amplitude of the near-tip fields, is independent of these size restrictions and is applicable over the range from small scale yielding to situations involving significant plastic deformation. Therefore, accurate values of J CAN be obtained by using the path integral approach in conjunction with specialized crack tip elements which impose the 1/r singularity in the strain energy density at the crack tip.

Although the present effort failed in the objective of calculating the J-integral directly as the amplitude of the plastic singular solution, the use of plastic singular elements at the crack tip was found to be beneficial for the evaluation of J about paths remote from the crack tip. Thus the only real limitations of the present effort toward the prediction of fracture are imposed by the restrictions on the use of the J-integral as a fracture criterion. Briefly, the J approach is limited to prediction of fracture initiation from a preexisting flaw. The J-integral serves to measure the amplitude of the near-tip field and, given its critical value,

---

*This may be seen by considering a limitingly small contour or path surrounding the crack tip. A lower order singularity in the strain energy density would lead to a limitingly small value of J on this path and a higher order singularity would result in increasingly large J path values.

to predict crack growth. This approach clearly presupposes the same failure mechanism in all situations where J is applicable. Thus, the scale of the plastic deformation prior to failure must be limited such that the mechanism is flat fracture and, for example, excludes ductile tearing.

REFERENCES

1. Henshell, R.D. and K.D. Shaw, "Crack-Tip Finite Elements are Unnecessary," International Journal for Numerical Methods in Engineering, Vol. 9, pp. 495-507 (1975).

2. Barsoum, R.S., "On the Use of Isoparametric Finite Elements in Linear Fracture Mechanics," International Journal for Numerical Methods in Engineering, Vol. 10, pp. 25-37 (1976).

3. Pu, S.L. and M.A. Hussain, "The Collapsed Cubic Isoparametric Element as a Singular Element for Crack Problems," International Journal for Numerical Methods in Engineering, Vol. 12, No. 11, pp. 1727-1742 (1978).

4. Hilton, P.D. et al., "Finite Element Fracture Mechanics Analysis of Two-Dimensional and Axisymmetric Elastic and Elastic-Plastic Cracked Structures," NSRDC Report 4493 (1974).

5. Gifford, L.N. and P.D. Hilton, "Stress Intensity Factors by Enriched Finite Elements," Engineering Fracture Mechanics, Vol. 10, pp. 485-496 (1978).

6. Gifford, L.N., "APES-Second Generation Two-Dimensional Fracture Mechanics and Stress Analysis by Finite Elements," DTNSRDC Report 4799 (1975).

7. Benzley, S.E., "Representation of Singularities with Isoparametric Finite Elements," International Journal for Numerical Methods in Engineering, Vol. 8, pp. 537-545 (1974).

8. Gifford, L.N., "APES-Finite Element Fracture Mechanics Analysis: Revised Documentation," DTNSRDC Report 79/023 (Mar 1979).

9. Hilton, P.D. and J.W. Hutchinson, "Plastic Intensity Factors for Cracked Plates," Engineering Fracture Mechanics, Vol. 3, pp. 435-451 (1971).

10. Hutchinson, J.W., "Singular Behavior at the End of a Tensile Crack in a Hardening Material," Journal of Mechanics and Physics of Solids, Vol. 16, No. 1 (1968).

11. Rice, J.R. and G.F. Rosengren, "Plane Strain Deformation Near a Crack Tip in a Hardening Material," Journal of Mechanics and Physics of Solids, Vol. 16, No. 1 (1968).

12. Rice, J.R., "Mathematical Analysis in the Mechanics of Fracture," in "Fracture," Vol. 2, Academic Press (1968).

13. Hilton, P.D., "Elastic-Plastic Analysis for Cracked Members," Trans. of ASME, Journal of Pressure Vessel Technology, Series J, Vol. 98, No. 1, pp. 47-55 (Feb 1976).

14. Barsoum, R.S., "Application of Quadratic Isoparametric Elements in Linear Fracture Mechanics," International Journal of Fracture, Vol. 10, pp. 603-605 (1974).

15. Benzley, S.E., "Nonlinear Calculations with a Quadratic Quarter-Point Crack Tip Element," International Journal of Fracture, Vol. 12, No. 3, pp. 475-477 (Jun 1976).

16. Wilson, W.K. and J.O. Osias, "A Comparison of Finite Element Solutions for an Elastic-Plastic Crack Problem," International Journal of Fracture, Vol. 14, pp. R95-R108 (1978).

INITIAL DISTRIBUTION

Copies		Copies	
1	DDR&E, Tech Lib	1	NADC
2	AMMRC 1 Library 1 Dr. T.P. Rich	1	NOSC
		1	NWC
2	WATERVLIET ARSENAL 1 Library 1 Dr. S.L. Pu	1	NCSC
		1	NSWC, White Oak
1	CNO, OP987 R&D Plans Div	1	NSWC, Dahlgren
4	CHONR 1 ONR 102 1 ONR 430 1 ONR 465 1 ONR 474	1	NUSC
		1	NAVAIR, 320
		1	NAVFAC, 03
3	NAVMAT 1 MAT 08E 1 MAT 08T1 1 MAT 08T23	1	CBC Port Hueneme CA CEL
		1	NAVSHIPYD CHASN
		1	NAVSHIPYD MARE
8	NRL 1 Code 6300 1 Code 6360 1 Code 6380 1 Code 6382 1 Code 6384 1 Code 8406 1 Code 8430 1 Code 8433	1	NAVSHIPYD PTSMH
		1	SUPSHIP GROTON
		1	SUPSHIP NEWPORT NEWS
		1	SUPSHIP PASCAGOULA
		12	DDC
4	NAVSEA 1 SEA 035 1 SEA 03511 1 SEA 03521 1 SEA 0353	1	ASD/ENFSF, WPAFB
		1	AFDL, WPAFB
		1	ASIAC (AFFDL/FBR)
1	USNA Dr. J.G. Joyce	2	BUSTAND, Boulder 1 Library 1 Dr. D.T. Read
1	NAVPGSCOL		
1	USNROTC & NAVADMIN, MIT		

Copies	
3	BUSTAND, Washington, D.C. 1 Library 1 Dr. R. DeWit 1 Dr. J.T. Fong
1	USCG
1	DOE, Oak Ridge
1	MARAD
1	NASA/Goddard
3	NASA/Langley 1 Library 1 Dr. R.E. Fulton 1 Dr. J.C. Newman
3	NASA/Lewis 1 Library 1 Dr. B. Gross 1 Dr. J.E. Strawley
1	NASA Scientific Tech Info Ofc
1	NUC Reg Comm 1 Library 1 Dr. J.R.N. Rajan
1	University of Arizona Dr. R.H. Gallagher
3	Battelle Memorial Institute 1 Library 1 Dr. G.T. Hahn 1 Dr. E.F. Rybicki
1	Boston University Dr. I. Fried
1	Brown University Dr. J.R. Rice
2	Carnegie-Mellon Inst 1 T.A. Cruse 1 Dr. J.L. Swedlow

Copies	
1	Colorado State Univ Dr. F.W. Smith
1	Univ of Connecticut Prof A.J. McEvily
1	Univ of Dayton Research Institute Dr. J.P. Gallagher
2	Franklin Institute 1 Library 1 Z. Zudans
2	George Washington Univ 1 J.D. Lee 1 A.K. Noor
1	Georgia Inst of Tech Dr. J.M. Anderson
1	Harvard Univ Dr. J.W. Hutchinson
2	Johns Hopkins Appl Phys Lab 1 Library 1 G. Daley
2	Lehigh Univ 1 Dr. G.C. Sih 1 Dr. R.P. Wei
1	Univ of Maryland Dr. G.R. Irwin
1	Univ of Massachusetts Dr. W.A. Nash
1	MIT Dr. K. Masabuchi
1	Michigan Tech Univ Dr. V.W. Snyder
1	Stanford Research Inst

Copies	
1	Southwest Research Inst J.R. Maison
1	VPI&SU Dr. G.W. Swift
4	Univ of Washington 1 APL 1 Dr. A.F. Emery 1 L. Hodulak 1 Dr. A.S. Kobayashi
2	Washington University 1 Dr. M. Gomez 1 Dr. P.C Paris
1	Yale Univ Dr. D.M. Parks
1	Air Products & Chemicals M.G. Zellner
1	Allis-Chalmers Corp H.R. Jhansale
1	ALCOA (Pitts) J.G. Kaufman
1	Babcock and Wilcox Research Center J.M. Bloom
2	Battelle Pacific Northwest 1 M.C.C. Bampton 1 G.H. Beeman
1	Bethlehem Steel Corp B.D. MacDonald
1	Boeing Aerospace Company (Seattle) A.V. Viswanathan
2	Brookhaven National Lab 1 Dr. M. Reich 1 D. Gardner

Copies	
1	Combustion Engineering Dr. R.S. Barsoum
1	General Dynamics Corp Electric Boat Div
2	General Electric Co (Schenectady) 1 Dr. C.F. Shih 1 W.R. Andrews
1	Ingalls Shipbldg Corp
1	Lockheed Palo Alto Res Lab
1	NNSB&DD Co
1	Northrop Corp (Hawthorne) J.R. Yamane
1	Oak Ridge National Laboratory S.K. Iskander
6	Sandia Laboratories (Albuquerque) 5 Dr. P.D. Hilton 1 Dr. S.E. Benzley
1	U.S. Steel Corp (Monroeville) J.M. Barsom
1	Welding Research Council
3	Westinghouse Elec Corp (Pittsburgh) 1 Dr. W.K. Wilson 1 Dr. D.E. McCabe 1 Dr. N.E. Dowling
1	Weston Components & Controls W.R. Hartman

CENTER DISTRIBUTION

Copies	Code	Name
1	11	
1	17	
1	1702	
1	1706S (m)	
1	1707	
2	172	
1	1720.1	
1	1720.2	
1	1720.3	
20	1720.4	
1	1720.5	
1	1720.6	
1	173	
1	1730.5	
1	1730.6	
1	174	
1	1740.5	
1	177	
1	177.7 (m)	
1	1805	
1	1844	
1	28	
1	2814	
1	282	
10	5211.1	Reports Distribution
1	522.1	Unclassified Lib (C)
1	522.2	Unclassified Lib (A)